

Flight-Level Thermodynamic Instrument Wetting Errors in Hurricanes. Part II: Implications

MATTHEW D. EASTIN

Department of Atmospheric Science, Colorado State University, Fort Collins, Colorado

PETER G. BLACK

Hurricane Research Division, NOAA/AOML, Miami, Florida

WILLIAM M. GRAY

Department of Atmospheric Science, Colorado State University, Fort Collins, Colorado

(Manuscript received 1 March 2001, in final form 5 October 2001)

ABSTRACT

The implications of flight-level instrument wetting error removal upon the mean thermodynamic structure across the eyewall, buoyancy of rainband vertical motions, and vertical energy fluxes near the top of the inflow layer are studied. Thermodynamic quantities across the mean eyewall are found to increase at all levels. As a result, maximum radial gradients of each quantity are shifted from the center of the eyewall cloud toward the outer edge. The increase in equivalent potential temperature lifts eyewall values to comparable magnitudes observed in the eye. The mean virtual potential temperature deviation of rainband updrafts increases from slightly negative to slightly positive. This increase and shift in sign are more pronounced in stronger updrafts. The mean deviation in rainband downdrafts decreases slightly toward neutral conditions. Vertical sensible heat fluxes near the top of the inflow layer are found to shift from downward to upward. Upward latent heat fluxes increase. Implications of these results upon hurricane structure and evolution are discussed.

1. Introduction

An understanding of how hurricane inner-core convection behaves and interacts with the vortex is important. The convection directly provides the latent heat release and vertical transport of mass and energy required to sustain the warm core structure. Any resulting feedbacks upon the local environment can affect both subsequent convection and storm evolution. These processes must be better understood before significant advancements in hurricane intensity prediction can be achieved (Elsberry et al. 1992). Numerous studies (e.g., Malkus and Riehl 1960; Gray 1965; Gray and Shea 1973; Barnes et al. 1983; Jorgensen 1984a,b; Jorgensen et al. 1985) have utilized flight-level observations to infer the nature of convection and its role in hurricane evolution. However, the evaluation of thermodynamic quantities was limited due to possible instrument wetting errors.

This paper is the second of two papers discussing

thermodynamic instrument wetting errors within flight-level data collected in the hurricane inner core. In the first paper (Eastin et al. 2002, hereafter Part I) salient features of significant instrument wetting errors were described and a statistical summary of error magnitudes was presented. To review, concurrent temperatures from a Rosemount immersion thermometer (which can suffer from wetting errors) and a modified Barnes radiometer (which is more accurate in clouds and precipitation) were compared to identify regions, called instrument wetting events (IWE), in which Rosemount temperatures were significantly cooler than radiometer-derived temperatures. IWE were found to frequently occur in the hurricane inner core. The majority of IWE were dominated by updrafts containing cloud drops and confined to convective length scales. As a result of these errors, thermodynamic quantities such as temperature (T), specific humidity (q), virtual potential temperature (θ_v), and equivalent potential temperature (θ_e) were typically underestimated by at least 1°C, 1 g kg⁻¹, 1 K, and 4 K, respectively. The correction method proposed by Zipser et al. (1981) was found to be only partially effective, removing 30%–50% of the error. This paper utilizes the same dataset to illustrate significant impacts

Corresponding author address: Matthew D. Eastin, Department of Atmospheric Science, Colorado State University, Fort Collins, CO 80523.

E-mail: eastin@mpi.atmos.colostate.edu

upon the mean thermodynamic structure across the eyewall, buoyancy of rainband vertical velocity cores, and vertical energy fluxes near the top of the inflow layer, once the errors are effectively removed. Part I should be consulted for a detailed discussion of the instrumentation, dataset, and analysis techniques.

2. Mean eyewall thermodynamic structure

Eyewall convection has long been recognized to play a fundamental role in hurricane evolution (e.g., Malkus and Riehl 1960). To improve our understanding of this role, the structure of eyewall convection and its interaction with the vortex need to be diagnosed with accurate kinematic and thermodynamic observations. As a first step, past studies (e.g., Shea and Gray 1973; Jorgensen 1984b) have diagnosed the mean eyewall structure from flight-level data. Shea and Gray (1973) argued that instrument wetting errors had an insignificant effect upon the mean thermodynamic structure. However, as shown in Part I, over 70% of IWE were associated with eyewall convection. Therefore, the mean eyewall thermodynamic radial structure was reexamined to determine if the removal of instrument wetting errors was significant.

In order to focus on eyewall convection, a radius of maximum updraft (RMU) was identified in the flight-level vertical velocity data of each radial leg as the maximum 0.5-km upward motion found within the eyewall. Radar imagery and profiles of horizontal wind and cloud water content (q_c) were used to help subjectively identify the primary eyewall. The vertical velocity (w) at the RMU was not required to satisfy the convective core criteria ($w > 1.0 \text{ m s}^{-1}$ for 0.5 km) used in Part I, but over 90% met this criteria. No RMU was identified for 28 radial legs in which downdrafts dominated the eyewall. These radial legs were not included in the analysis, and their absence does not affect the conclusions. The average RMU is located 26 km from the storm center [with a standard deviation (σ) of 12.2 km], or ~ 4 km inside the radius of maximum wind (RMW) toward the inner edge of the eyewall. The average location of the RMU is consistent with Jorgensen (1984a). Note that use of the RMU, rather than the commonly used RMW, acts to remove any radial variability between the RMW and eyewall convection while maintaining focus upon the convection.

The mean thermodynamic structure across the eyewall was evaluated by first calculating the environmental temperature deviation (ΔT), q , and θ_e along each radial leg, and then compositing the profiles with respect to the eyewall RMU. Environmental temperature deviations were determined by subtracting the mean temperature at RMW + 10 km (i.e., outside the eyewall to 150 km) from the observed temperature. Values of θ_e were calculated using the Bolton (1980) formulation. In order to determine the effects of instrument wetting error removal, the compositing method was separately

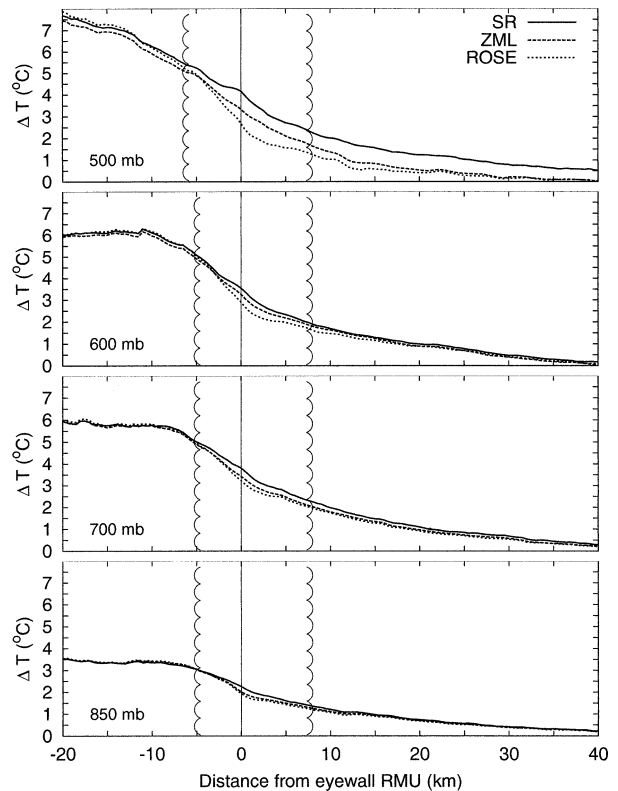


FIG. 1. Composite profiles of environmental temperature deviation (ΔT) across the eyewall at 850, 700, 600, and 500 mb. The composites were constructed from all hurricane radial legs by positioning SR (solid), ZML (dashed), and ROSE (dotted) data with respect to the eyewall RMU of each leg. A negative distance is radially inward from the eyewall RMU (toward the eye). Vertical scalloped lines mark the inner and outer edges of the composite eyewall cloud (defined by $q_c > 0.2 \text{ g m}^{-3}$). See text for definition of environmental temperature deviations and the eyewall RMU.

applied to the radial profiles of temperature and dewpoint constructed from radiometer and hygrometer data, Rosemount thermometer and hygrometer data, and Rosemount thermometer and hygrometer data corrected using the ZML method (hereafter, the SR, ROSE, and ZML data, respectively). In addition, the edges of the mean eyewall cloud were identified at each level as the locations where mean q_c (composited in a similar manner) exceeded 0.2 g m^{-3} . The resulting composite profiles are representative of an eyewall in a steady-state mature hurricane with IWE in $\sim 35\%$ of the radial legs. It will be shown that the removal of such few IWE has a significant effect upon the mean thermodynamic structure.

The warm core structure of a hurricane is well depicted by the composite ΔT profiles shown in Fig. 1. Environmental temperature deviations decrease with radius from a maximum near the storm center, and increase with height. The SR, ROSE, and ZML average ΔT within the eye (and outside the eyewall) are in good agreement, and the observed mean values are consistent with Shea and Gray (1973). However, inside the eyewall

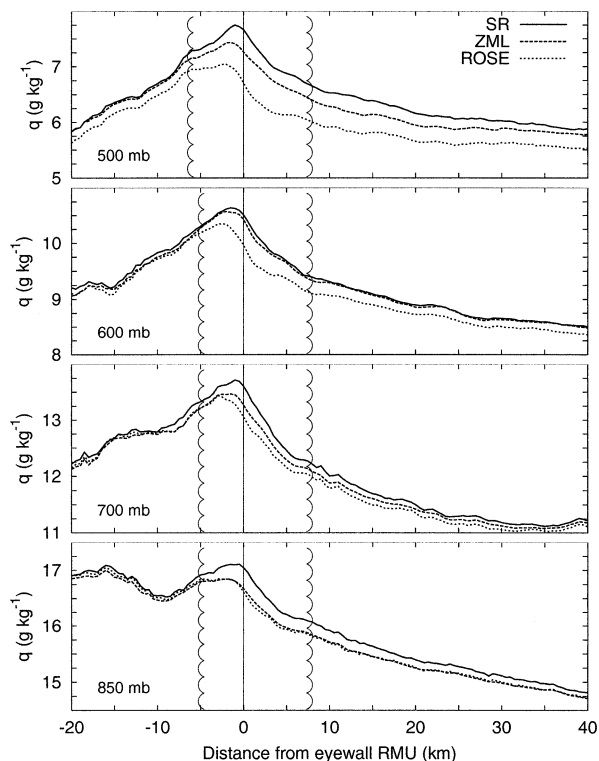


FIG. 2. Similar to Fig. 1 but for specific humidity (q).

cloud, instrument wetting errors (depicted by the ROSE and ZML profiles compared to the SR profiles) act to underestimate mean ΔT by 0.5° – 1.0° C. This underestimation increases with height due to both an increase in q_e with height, and additional cooling effects induced by ice near the freezing level (~ 500 mb). The large errors outside the eyewall at 500 mb are believed to result from a buildup of ice on the sensor. The net effect of instrument wetting error removal on ΔT was to shift the maximum radial temperature gradient toward the eyewall outer edge.

The mean moisture structure across the eyewall is depicted by the composite q profiles shown in Fig. 2. Maximum specific humidity is found in the eyewall at each level. Strong radial gradients extend from the eyewall in both directions, resulting in suppressed q in the eye above 850 mb. The weak radial gradient between the eye and eyewall at 850 mb is indicative of the moist air commonly found in the eye beneath an inversion below 700 mb (e.g., Jordan 1961). The local minimum 10 km inside the RMU is a result of sporadic forced descent along the inner edge of the eyewall (Jorgensen 1984b). These profiles are qualitatively consistent with the inner-core q structure presented in Hawkins and Rubsam (1968) and Hawkins and Imbembo (1976). Again, comparison between the SR, ROSE, and ZML data demonstrates that mean q values agree better in the eye than inside the eyewall, where instrument wetting errors result in an underestimation of q by 0.4 – 0.8 g kg^{-1} .

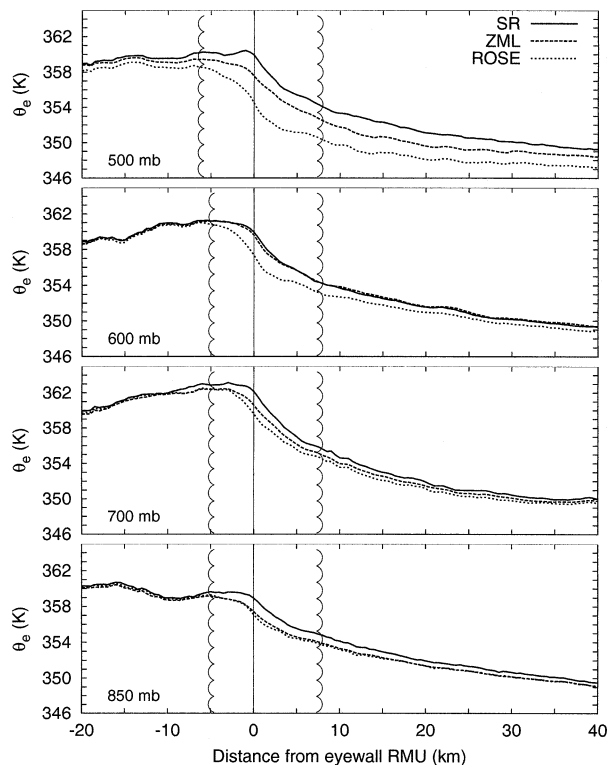


FIG. 3. Similar to Fig. 1 but for equivalent potential temperature (θ_e).

The net effects of error removal on q are to shift the radial maximum from near the inner edge of the eyewall toward the RMU, and to shift the maximum radial gradient toward the outer edge.

The mean θ_e structure across the eyewall is shown in Fig. 3. Maximum values are found in either the eye or eyewall. Radial gradients well outside the eyewall and between the eye and eyewall are weak. Vertical variations are small at all radii. The profiles are in qualitative agreement with the θ_e cross section presented in Hawkins and Imbembo (1976), except that no significant θ_e minimum was found at midlevels in the eye. Again, agreement between the SR, ROSE, and ZML profiles in the eye is good, but the presence of instrument wetting errors within the eyewall data act to underestimate mean θ_e by 3–5 K. Thus, the net effect of error removal was to shift the maximum radial gradient of θ_e from across the eyewall RMU toward the eyewall outer edge, and to elevate θ_e values at the RMU to comparable values found in the eye.

The impact of instrument wetting error removal upon the mean thermodynamic structure across the eyewall can be further illustrated by examining data from a single flight. Shown in Fig. 4 are the composite profiles of ΔT , q , and θ_e constructed in a similar manner from the 12 radial legs flown at 500 mb in Hurricane Guillermo between 1855 UTC 3 August and 0041 UTC 4 August 1997. During this time, Guillermo was near the

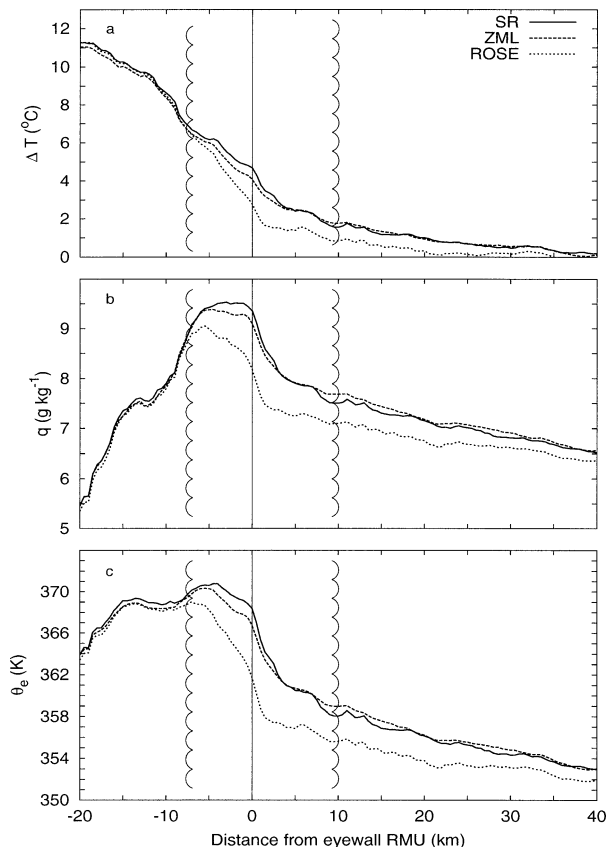


FIG. 4. Composite profiles of (a) environmental temperature deviation ΔT , (b) specific humidity q , and (c) equivalent potential temperature θ_e , across the eyewall of Hurricane Guillermo at 500 mb during the period between 1855 UTC 3 Aug and 0041 UTC 4 Aug 1997. The profiles were constructed from the 12 radial legs obtained during the observation period. An instrument wetting event was identified in 11 out of 12 radial legs during passage through eyewall convection. Vertical scalloped lines mark the inner and outer edges of the composite eyewall cloud (defined by $q_e > 0.2 \text{ g m}^{-3}$).

end of a 48-h intensification period from a minimal category 1 to an intense category 5 hurricane. The average RMU was at 26 km ($\sigma = 2.4 \text{ km}$), and 11 out of 12 radial legs contained IWE in the eyewall. The composite structures are similar to those shown in Figs. 1–3 for 500 mb, with the exception of an enhanced radial θ_e gradient 15 km inside the RMU that suggests that a local θ_e minimum was located near the center of Guillermo's eye at this time. The removal of instrument wetting errors increased the mean ΔT , q , and θ_e values across the eyewall by 2°C , 1 g kg^{-1} , and 6 K , respectively. Again, maximum radial gradients of each quantity were shifted toward the outer edge of the eyewall cloud. These profiles illustrate the effect that IWE can have upon the mean thermodynamic structure of a single eyewall, and demonstrate that future case studies of hurricane convection should utilize radiometric data.

The effects of instrument wetting error removal upon mean eyewall structure may appear small, but are not trivial. First, Eastin (1999) showed that thermal wind

imbalances near the RMW were reduced by $\sim 50\%$ when errors were removed. This suggests that the *mean* vortex may be more in balance (hydrostatic and gradient wind) than some studies (e.g., Gray and Shea 1973) have previously diagnosed. Second, the small vertical θ_e variations at the eyewall RMU imply that the *mean* profile is moist adiabatic to a first approximation.¹ This has implications upon entrainment and any conditional instability in the eyewall. Finally, the increase in θ_e at the RMU to nearly equivalent values observed in the eye and eyewall takes place in the lower and middle troposphere. Each of the above implications influence our conceptual understanding of how hurricanes evolve. We shall now explore the latter implication more.

Malkus (1958) and Kuo (1959) argued that frequent inward mixing of eyewall air is required through a deep layer to force subsidence in the eye and maintain thermodynamic and momentum budgets. Willoughby (1998) recently proposed a contrasting conceptual model of hurricane evolution, based upon eyewall contraction and small vertical displacements of eye air, in order to explain observed changes in eye thermodynamics. In this model, the eye consists of two distinct air masses separated by an inversion between 850 and 700 mb. The air below the inversion mixes freely with eyewall. The air above the inversion consists of a "plug" of air that is captured when the eyewall initially develops and remains isolated from the eyewall (i.e., little or no mixing occurs with the eyewall) while experiencing only small vertical displacements. Therefore, the θ_e properties within the midlevel eye are determined at eyewall formation and remain nearly constant until eyewall dissipation. As a result, this conceptual model predicts θ_e differences of 10 K or more between the eye and eyewall above 700 mb in intense hurricanes.

The composite θ_e profiles (Fig. 3) do not support substantially elevated maxima in the mean eyewall. Inspection of individual radial legs, however, indicates that periods exist during which eyewall θ_e is enhanced and eye θ_e is suppressed. The composite profile for Guillermo (Fig. 4c) is one such case. Kossin and Eastin (2001) recently presented observational evidence that horizontal mixing of eyewall θ_e maximum into the eye occasionally occurs during intensification and frequently occurs over the course of a few hours just after maximum intensity. The composite profiles cannot provide temporal information regarding the mixing, but do provide further support that substantial mixing between the

¹ The use of flight-level data to deduce vertical variations must be done with extreme caution. In this case, a composite mean value at a given level was calculated from data obtained in different storms and environments. Therefore, small perturbations upon this representative mean structure are likely due to the variability of the data used to construct the composite and not representative of the mean vertical gradients within any given storm.

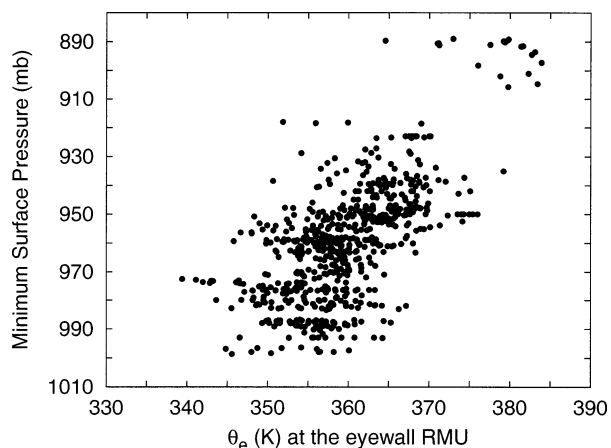


FIG. 5. Scatterplot of equivalent potential temperature (θ_e) calculated from SR data at the eyewall RMU. Minimum surface pressures were obtained from the best track database. See text for definition of the eyewall RMU.

eye and eyewall must occur on timescales much smaller than the complete evolution of a hurricane.

On a final note concerning eyewall thermodynamics, it was shown that mean θ_e values increase significantly once instrument wetting errors are removed, and that θ_e can increase by ~ 10 K or more within individual IWE (see Part I). However, the variability of actual θ_e values in the eyewall has yet to be addressed. Figure 5 presents a scatterplot of θ_e calculated from SR data at the RMU of each radial leg. These values represent the most accurate flight-level measurements of θ_e available to date. Values range from 339 to 384 K and tend to increase with storm intensity. The range at a given intensity is ~ 20 K. This latter range represents either temperature variations of $\sim 5^\circ\text{C}$, specific humidity variations of ~ 6 g kg $^{-1}$, or some combination of the two. It is interesting to note that such T and q variations are consistent with their observed variability across the mean eyewall (Figs. 1 and 2) and in the hurricane boundary layer (Cione et al. 2000).

3. Buoyancy of rainband convection

The vertical transport of mass, momentum, heat, and moisture plays an important role in the energy balance and evolution of hurricanes. Jorgensen et al. (1985) showed that the majority of the vertical mass transport is accomplished by convective scale updrafts and downdrafts. However, the variety of forcing mechanisms that can drive convective vertical motions are not well understood or documented within hurricanes. One such mechanism is buoyancy. Ooyama (1982) argues that cloud buoyancy is required to intensify a hurricane, while Gray (1997) argues that substantial buoyancy is also required for maintenance. In contrast, Emanuel (1986) argues that cloud buoyancy plays a secondary role in hurricane evolution as moist convection ap-

proaches a neutral state in mature storms. Zhang et al. (2000) further argue that the vertical perturbation pressure gradient significantly contributes to driving upward vertical motions. One reason the debate remains unsettled is that accurate magnitudes of buoyancy have been difficult to obtain due to possible instrument wetting errors that are of the same magnitude as typical buoyancy values (Gray 1965; Jorgensen et al. 1985; Part I). Therefore, buoyancy magnitudes within rainband updrafts and downdrafts were examined to determine the effects of instrument wetting error removal upon such calculations and to provide the first accurate estimates within hurricane convection.

We define the buoyancy ($\Delta\theta_v$) of convective vertical motions as

$$\Delta\theta_v = \theta_v - \theta_{ve}, \quad (1)$$

where the subscript e refers to a local environment. The effects of water loading and perturbation pressure are neglected. As in Part I, analysis is confined to updraft and downdraft cores ($|w| > 1.0$ m s $^{-1}$ for 0.5 km), which contain cloud water ($q_c > 0.0$ g m $^{-3}$). The environment of each core was assumed to be locally represented by the arithmetic mean of all θ_v within 20 km (± 10 km from the core edges). This environmental definition may not be representative in the presence of strong, large-scale thermodynamic gradients (such as in the eyewall). Therefore, analysis is further confined to the rainband region where large-scale radial gradients are weak. A total of 418 updraft and 170 downdraft cores were identified within the rainband convection located between ~ 45 and 150 km from the storm center. Several characteristics of each core were tabulated. These include average w , q_c , and $\Delta\theta_v$, extreme w and $\Delta\theta_v$, and diameter (or radial distance along the flight track). Extreme w and $\Delta\theta_v$ are the maximum (minimum) 0.5-km values in the updraft (downdraft) cores. Values of $\Delta\theta_v$ were calculated from each of the SR, ROSE, and ZML data. Rainband convection is believed to be well represented since the distributions of core diameter and w (not shown) are consistent with Jorgensen et al. (1985). It should be further noted that this dataset represents all stages of growing, mature, and dissipating convection.

Shown in Fig. 6 are the distributions of average $\Delta\theta_v$ across updraft cores as determined from SR, ZML, and ROSE data. Each are approximately normally distributed. The removal of instrument wetting errors shifted the mean $\Delta\theta_v$ from roughly -0.20 to $+0.15$ K. This shift is statistically significant at the 99% level (according to a t test). Furthermore, the cumulative percentage of average $\Delta\theta_v$ in excess of 0.5 K increases from $\sim 5\%$ to $\sim 25\%$. Application of the ZML method only increased the mean $\Delta\theta_v$ to a statistically insignificant $+0.08$ K indicative of neutral convection. Therefore, the removal of instrument wetting errors elevated average $\Delta\theta_v$ values such that a significant fraction of updrafts may be active convection. It is interesting to

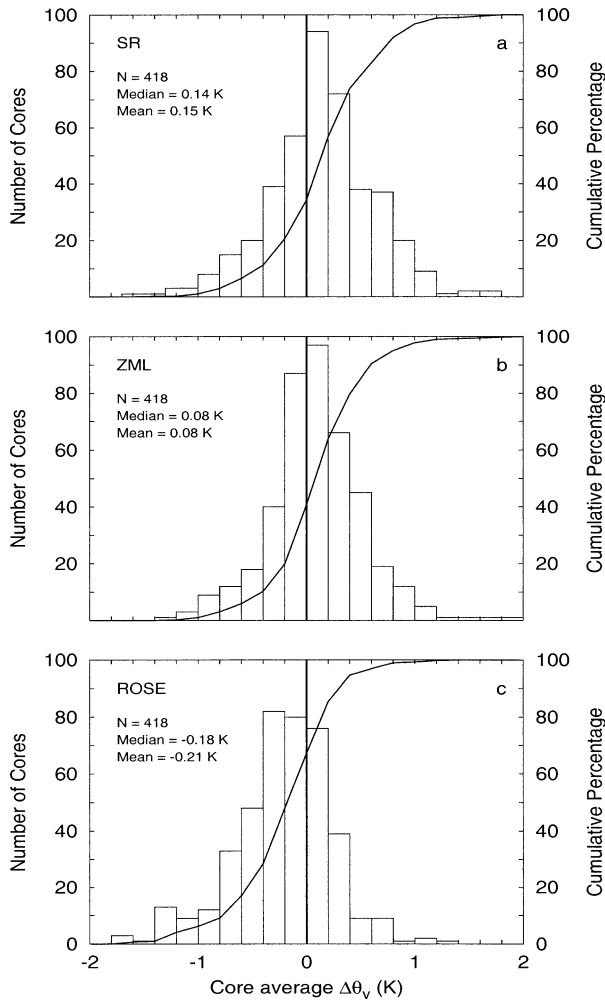


FIG. 6. Histograms of average virtual potential temperature deviation ($\Delta\theta_v$) in rainband updraft cores containing cloud water as determined from (a) SR, (b) ZML, and (c) ROSE data. Solid lines represent the cumulative percentage of each distribution. The variable N is the total number of cores.

note that the corrected $\Delta\theta_v$ distribution (Fig. 6a) for hurricane rainbands is in qualitative agreement with the $\Delta\theta_v$ distributions observed in other tropical oceanic convection (Jorgensen and LeMone 1989; Lucas et al. 1994; Wei et al. 1998).

The effects of error removal are further illustrated when the respective average $\Delta\theta_v$ is presented as a function of vertical velocity. Figure 7 indicates that the majority of strong updrafts ($w > 3.0 \text{ m s}^{-1}$) are negatively buoyant when $\Delta\theta_v$ is calculated from the ROSE data. In contrast, calculation of $\Delta\theta_v$ from the SR data results in positive buoyancy for the majority of strong updrafts. Parcel theory predicts that active updrafts will have a positive correlation between average $\Delta\theta_v$ and updraft strength. The SR data supports such a relationship, but the ROSE data does not.

Figure 8 shows the distributions of average $\Delta\theta_v$ across downdraft cores. Again, each are approximately

normally distributed. The removal of instrument wetting errors slightly decreased the mean $\Delta\theta_v$ from $+0.14$ to $+0.03 \text{ K}$, indicative of neutral conditions. Application of the ZML method resulted in a similar $\Delta\theta_v$ reduction. These changes are primarily a result of error removal from core environments that act to increase θ_{ve} and decrease $\Delta\theta_v$. The positive mean $\Delta\theta_v$ in downdrafts is consistent with previous studies in tropical oceanic convection (Jorgensen and LeMone 1989; Lucas et al. 1994; Wei et al. 1998; Igau et al. 1999).

What do the observed $\Delta\theta_v$ magnitudes suggest about hurricane rainband convection once instrument wetting errors are removed? Parcel theory predicts that positive (negative) $\Delta\theta_v$ will accelerate air upward (downward) in the absence of water loading and nonhydrostatic pressure forces. The accelerations can be significant for relatively small $\Delta\theta_v$ values. For example, an air parcel initially at rest in the lower troposphere with a $\Delta\theta_v$ of 0.2 K will accelerate to $\sim 8 \text{ m s}^{-1}$ over 5 km . As a result, several recent studies (e.g., Lucas et al. 1994) attempting to explain observed vertical velocities have argued that water loading plays a significant role in reducing buoyancy. Water loading could effectively drive warm downdrafts since only moderate liquid water contents would be required. In contrast, warm updrafts must overcome water loading in order to accelerate upward. Observations of liquid water contents indicate that total values rarely exceed 1.5 g m^{-3} in hurricanes (Ackerman 1963; Jorgensen et al. 1985; Black and Hallett 1986). Since 1.5 g m^{-3} would reduce a $\Delta\theta_v$ of only 0.5 K to zero, one could speculate that a significant fraction of hurricane rainband updraft cores are buoyant. Direct observations of total liquid water content were not available to test this speculation, but several other factors support such a statement. Figures 7a and 7b indicate that strong updrafts have greater positive $\Delta\theta_v$ than weaker updrafts. Stratification of the updrafts by flight level (Table 1) indicates that average and extreme $\Delta\theta_v$ tend to increase with height to maxima of 0.3 and 0.6 K , respectively, at 600 mb . Linear correlation coefficients between w and $\Delta\theta_v$ also increase with height to a maximum of 0.52 at 600 mb . Although these results are circumstantial, the evidence suggests that a significant fraction of hurricane rainband updraft cores are indeed buoyant. Furthermore, Bogner et al. (2000) evaluated the convective available potential energy (CAPE) in six hurricanes with dropsonde data and found that the rainband region could support buoyant convection.

4. Vertical fluxes near the top of the inflow layer

The thermodynamic structure and evolution of the hurricane inflow layer has long been recognized to play a crucial role in hurricane evolution. Early studies focused on the energetics of the subcloud layer (below $\sim 500 \text{ m}$) and speculated that isothermal inflow is maintained against adiabatic and evaporative cooling by heat transfer from the sea and downward heat fluxes at cloud

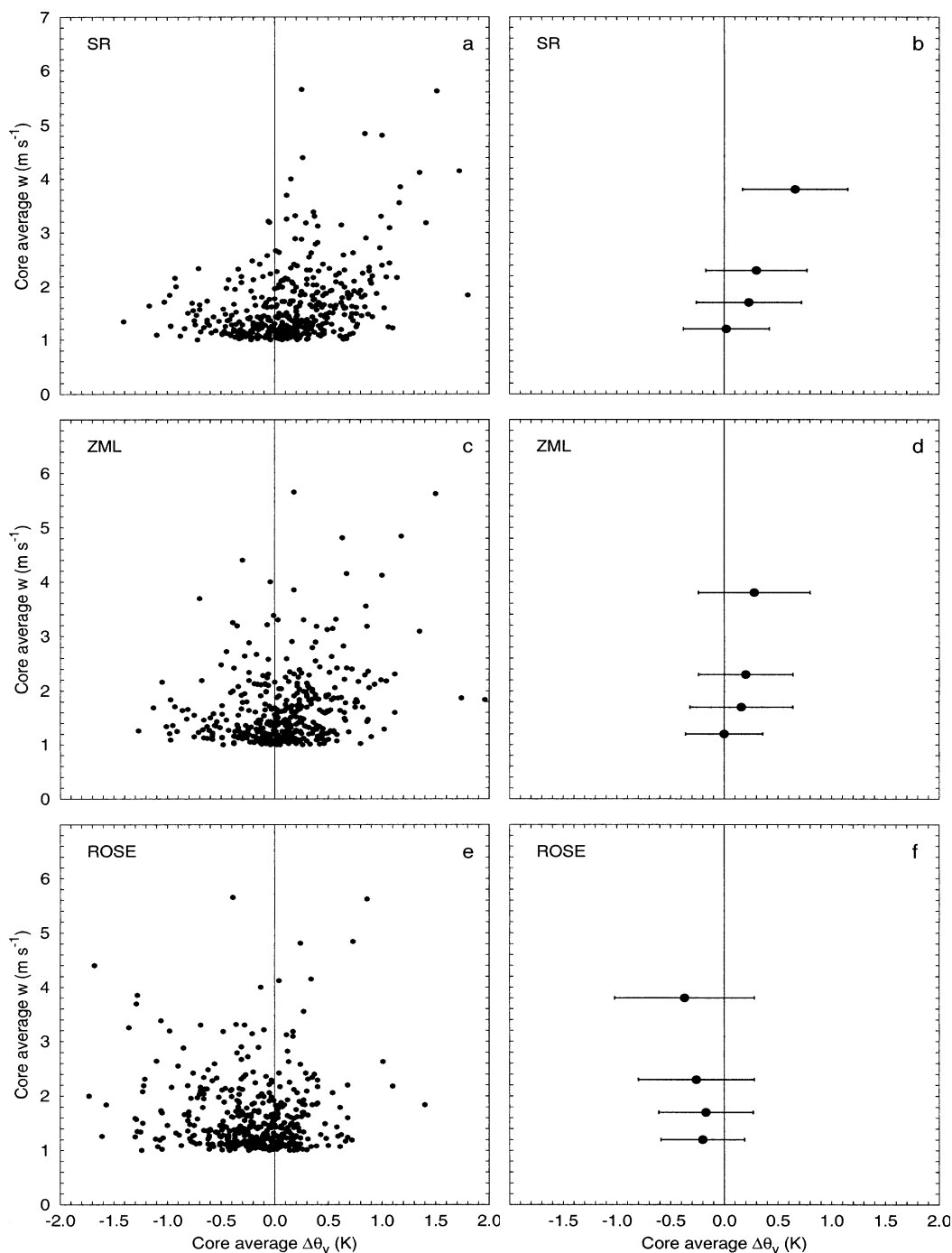


FIG. 7. Scatterplots of average virtual potential temperature deviation $\Delta\theta_v$ versus average vertical velocity w in rainband updraft cores containing cloud water as determined from (a) SR, (c) ZML, and (e) ROSE data. Means of average $\Delta\theta_v$, taken over specified w intervals are shown in the right-hand panels for the (b) SR, (d) ZML, and (f) ROSE data. Error bars represent one standard deviation from the mean. The w intervals ($1.0 \leq w \leq 1.5 \text{ m s}^{-1}$; $1.5 < w \leq 2.0 \text{ m s}^{-1}$; $2.0 < w \leq 3.0 \text{ m s}^{-1}$; and $w > 3.0 \text{ m s}^{-1}$) contained 238, 94, 62, and 23 cores, respectively.

base (Byers 1944; Malkus and Riehl 1960; Frank 1977, 1984; Anthes and Chang 1978; Riehl 1981; Betts and Simpson 1987). More recent studies focused on the energetics of the entire inflow layer (primarily below $\sim 1500 \text{ m}$) and have suggested that the isothermal con-

ditions near the surface can be significantly disrupted by cool, dry convective downdrafts that penetrate into the inflow layer (Barnes et al. 1983; Powell 1990). As a result, storm intensity could be affected if the modified inflow cannot recover prior to reaching the eyewall.

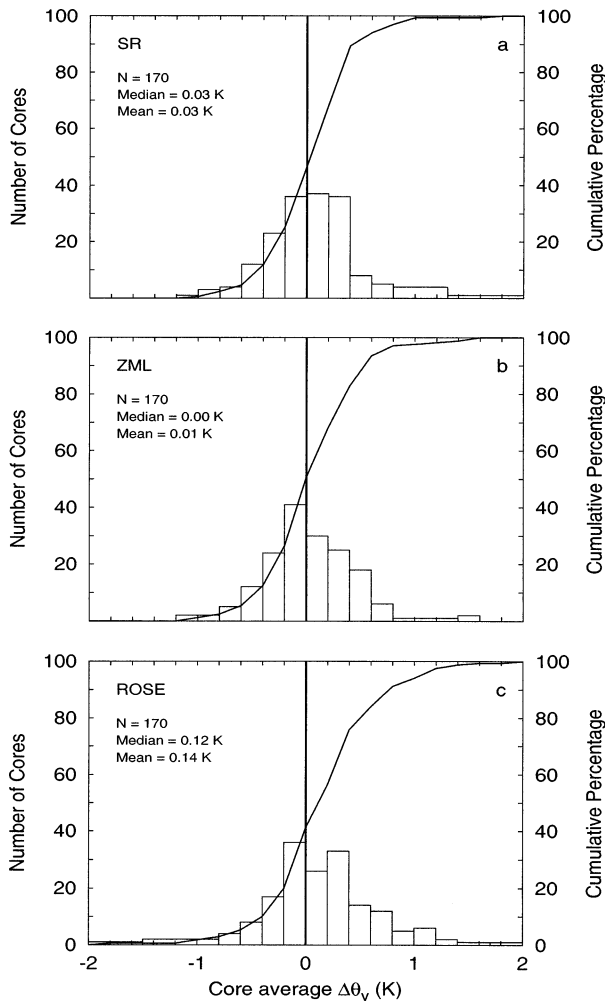


FIG. 8. Similar to Fig. 6 but for rainband downdraft cores.

Frank (1984) has been the only study to directly document vertical sensible heat fluxes near the top of the inflow layer with flight-level data. He found average convective fluxes in the region outside the eyewall (between 60 and 140 km from the storm center) to be directed *downward* across the 1600-m level with a mag-

nitude of 50 W m^{-2} . However, instrument wetting errors were not explicitly accounted for in the calculations, and any such error collocated with an updraft could lead to an erroneous downward flux. Therefore, vertical heat and moisture fluxes near the top of the inflow layer were reexamined to determine the effects of instrument wetting errors upon their magnitude and sign.

The total vertical flux of sensible and latent heat across a level, divided into mean transport and convective flux terms, are defined as

$$\rho c_p \overline{\theta w} = \rho c_p \overline{\theta} \overline{w} + \rho c_p \overline{\theta' w'} \quad (2)$$

$$\rho L \overline{q w} = \rho L \overline{q} \overline{w} + \rho L \overline{q' w'}, \quad (3)$$

where ρ is the leg average density calculated from the equation of state, c_p is the specific heat of air at constant pressure, L is the latent heat of vaporization, and θ is potential temperature. Overbars represent means over 20 km, and primes represent perturbations from the means. In order to concentrate on fluxes near the top of the inflow layer, analysis was confined to the 850-mb (~ 1500 m) level and the rainband region located ~ 45 to 150 km from the storm center. The mean transport and convective flux terms are independently evaluated following the methods of Black and Holland (1995) to represent the average total flux across flight level. First, a 20-km running Bartlett filter was applied to the w , θ , and q data of each radial leg. The resulting low-pass-filtered data was then subtracted from the 0.5-km data to produce the high-pass-filtered data, and each series was de-trended. Next, the low-pass-filtered data was used to calculate mean transports on scales greater than 20 km, and the high-pass-filtered data was used to calculate convective, or cloud, fluxes on scales between 0.5 and 20 km. The positive and negative covariances for all segments were integrated separately and averaged to obtain the upward and downward fluxes. Finally, net mean transports, convective fluxes, and total fluxes were then computed from the upward and downward components. It should be noted that use of 0.5-km-resolution data may underestimate the convective flux magnitudes by a factor of 2 (Moss 1978). Latent heat fluxes may

TABLE 1. Mean and median (50%) values of average and extreme virtual potential temperature deviation ($\Delta\theta_v$) calculated from SR data in rainband vertical velocity cores containing cloud water. The extreme values represent the maximum (minimum) 0.5-km deviation in updraft (downdraft) cores. Bold mean values indicate statistical significance at the 99% confidence level. See text for vertical velocity core definition.

	Level (mb)	Number	Average $\Delta\theta_v$ (K)		Extreme $\Delta\theta_v$ (K)	
			Mean	50%	Mean	50%
Updraft cores	500	97	0.06	0.02	0.34	0.25
	600	91	0.30	0.27	0.57	0.53
	700	145	0.15	0.17	0.37	0.36
	850	85	0.09	0.10	0.20	0.15
Downdraft cores	500	39	0.05	-0.02	-0.08	-0.09
	600	24	-0.16	-0.16	-0.25	-0.26
	700	66	0.09	0.10	-0.04	0.01
	850	41	-0.01	-0.01	-0.08	-0.09

TABLE 2. Summary of average net vertical convective flux (scales less than 20 km), mean transport (scales greater than 20 km), and total flux of sensible and latent heat across 850 mb in the rainband region as determined from SR, ZML, and ROSE data.

Data type	Parameter	Sensible heat ($W m^{-2}$)	Latent heat ($W m^{-2}$)
SR	Convective flux	8.7	47.4
	Mean transport	9.3	22.7
	Total flux	18.0	70.2
ZML	Convective flux	-1.3	34.7
	Mean transport	2.4	13.9
	Total flux	1.1	48.7
ROSE	Convective flux	-14.8	13.2
	Mean transport	-10.1	1.0
	Total flux	-24.9	12.2

also be further underestimated due to the slow dewpoint sensor response time.

Shown in Table 2 are the resulting average vertical sensible and latent heat fluxes calculated from the SR, ZML, and ROSE data. A downward convective sensible heat flux on the order of $15 W m^{-2}$ prevails when instrument wetting errors are not removed. Such a flux is qualitatively consistent with Frank (1984). The mean transport is also directed downward with a similar magnitude, resulting in a total downward flux of $25 W m^{-2}$. Error removal, however, results in a total *upward* flux of $20 W m^{-2}$ as mean transports and convective fluxes are equally affected. Furthermore, total upward latent heat fluxes increase by $60 W m^{-2}$ when errors are removed. Application of the ZML method results in no appreciable net sensible heat flux across 850 mb and only a $30 W m^{-2}$ increase in the total latent heat flux. Therefore, instrument wetting error removal results in an increased net vertical export of both heat and moisture from the inflow layer.

To the extent that vertical fluxes calculated at 850 mb are representative of the top of the inflow layer, what do these results suggest about inflow layer energetics? Since the values presented in Table 2 are averages, these upward net fluxes of both heat and moisture appear to be prevalent in an "average" hurricane. The fluxes act to cool and dry the inflow layer through a combination of warm, moist updrafts and cold, dry downdrafts. The $\Delta\theta_v$ values presented in Table 1 lend support to such a process at 850 mb. The results also support the Barnes et al. (1983) hypothesis that the hurricane inflow layer can be significantly cooled by convective downdrafts and that hurricane structure and evolution may be closely related to the distribution of inflow cooling via convective processes.

5. Summary and concluding remarks

Flight-level data collected during 79 flights into 31 hurricanes were used to examine significant implications of instrument wetting errors upon hurricane thermodynamics. The effective removal of such errors through

the use of a radiometric thermometer was found to impact the mean thermodynamic structure across the eyewall, buoyancy of rainband convection, and vertical energy fluxes near the top of the inflow layer. Specific results upon error removal are

- 1) Average thermodynamic quantities across the eyewall increased at all levels. In particular, the temperature, specific humidity, and equivalent potential temperature increased by $\sim 1^\circ C$, $\sim 0.5 g kg^{-1}$, and $\sim 4 K$, respectively. As a result, the maximum radial gradients of each quantity shifted from the middle of the eyewall cloud toward the outer edge. The increase in equivalent potential temperature elevated eyewall values to comparable magnitudes found in the eye.
- 2) Average virtual potential temperature deviations increased in rainband updraft cores and decreased slightly in downdraft cores. The increase in updraft cores shifted the distribution mean from a slightly negative value ($-0.21 K$) to a slightly positive value ($+0.15 K$) indicative of buoyant convection. This increase was more pronounced in stronger updrafts, resulting in a moderate positive correlation between virtual potential temperature deviation and updraft strength. Consideration of typical liquid water contents observed in hurricane convection demonstrates that water loading would not effectively reduce the positive temperature deviations within a considerable fraction of updraft cores to zero.
- 3) Average vertical sensible heat fluxes near the top of the inflow layer reversed from downward to upward with a net increase of $50 W m^{-2}$. Upward latent heat fluxes increased by $\sim 60 W m^{-2}$. This net export of energy from the hurricane inflow is accomplished through a combination of warm, moist updrafts and cool, dry downdrafts.

This study explored only a few implications of instrument wetting errors. More fundamental research addressing hurricane convection and its interactions within the primary circulation is needed now that more accurate thermodynamic data are available. As we gain a better understanding of the adverse and beneficial effects induced by convection upon the hurricane vortex, we will undoubtedly improve our ability to forecast intensity changes. Presently, this unique dataset is being utilized to further investigate the thermodynamic characteristics of convective vertical velocity cores. In particular, magnitudes of vertical energy fluxes and buoyancy are being examined in the eyewall and related to storm structure, asymmetries, and evolution.

Acknowledgments. The authors would like to thank Jim Kossin, Joe Cione, and Ed Zipser for helpful discussions during the course of this work. The comments and suggestions of two anonymous reviewers were very beneficial. Jill Scheafer's editorial suggestions are appreciated. The first author would like to express his

gratitude to Dr. Hugh Willoughby and the entire Hurricane Research Division for allowing him the opportunity to participate in the field program over the past few years. This research was partially supported by NSF Grant ATM-9616818.

REFERENCES

- Ackerman, B., 1963: The distribution of liquid water in hurricanes. National Hurricane Research Project Report 62, U.S. Weather Bureau, 41 pp.
- Anthes, R. A., and S. W. Chang, 1978: Response of the hurricane boundary layer to changes in sea surface temperature in a numerical model. *J. Atmos. Sci.*, **35**, 1240–1255.
- Barnes, G. M., E. J. Zipser, D. Jorgensen, and F. Marks Jr., 1983: Mesoscale and convective structure of a hurricane rainband. *J. Atmos. Sci.*, **40**, 2127–2137.
- Betts, A. K., and J. S. Simpson, 1987: Thermodynamic budget diagrams for the hurricane subcloud layer. *J. Atmos. Sci.*, **44**, 842–849.
- Black, P. G., and G. J. Holland, 1995: The boundary layer of Tropical Cyclone Kerry (1979). *Mon. Wea. Rev.*, **123**, 2007–2028.
- Black, R. A., and J. Hallett, 1986: Observations of the distribution of ice in hurricanes. *J. Atmos. Sci.*, **43**, 802–822.
- Bogner, P. B., G. M. Barnes, and J. L. Franklin, 2000: Conditional instability and shear for six hurricanes over the Atlantic Ocean. *Wea. Forecasting*, **15**, 192–207.
- Bolton, D., 1980: The computation of equivalent potential temperature. *Mon. Wea. Rev.*, **108**, 1046–1053.
- Byers, H. R., 1944: *General Meteorology*. McGraw-Hill, 645 pp.
- Cione, J. J., P. G. Black, and S. H. Houston, 2000: Surface observations within the hurricane environment. *Mon. Wea. Rev.*, **128**, 1550–1561.
- Eastin, M. D., 1999: Instrument wetting errors in hurricanes and a re-examination of inner-core thermodynamics. Dept. Atmospheric Science Paper 683, Colorado State University, Fort Collins, CO, 203 pp. [Available from Dept. Atmospheric Science, Colorado State University, Fort Collins, CO 80523.]
- , P. G. Black, and W. M. Gray, 2002: Flight-level instrument wetting errors in hurricanes. Part I: Observations. *Mon. Wea. Rev.*, **130**, 825–841.
- Elsberry, R. L., G. J. Holland, H. Garrish, M. DeMaria, and C. P. Gaurd, 1992: Is there any hope for tropical cyclone intensity change prediction?—A panel discussion. *Bull. Amer. Meteor. Soc.*, **73**, 264–275.
- Emanuel, K. A., 1986: An air–sea interaction theory for tropical cyclones. Part I: Steady-state maintenance. *J. Atmos. Sci.*, **43**, 585–604.
- Frank, W. M., 1977: The structure and energetics of the tropical cyclone. I. Storm structure. *Mon. Wea. Rev.*, **105**, 1119–1135.
- , 1984: A composite analysis of the core of a mature hurricane. *Mon. Wea. Rev.*, **112**, 2401–2420.
- Gray, W. M., 1965: Calculations of cumulus draft velocities in hurricanes from aircraft data. *J. Appl. Meteor.*, **4**, 463–474.
- , 1997: The tropical cyclones Maximum Potential Intensity (MPI). Preprints, *22d Conf. on Hurricanes and Tropical Meteorology*, Fort Collins, CO, Amer. Meteor. Soc., 288–289.
- , and D. J. Shea, 1973: The hurricane's inner core region. II. Thermal stability and dynamic characteristics. *J. Atmos. Sci.*, **30**, 1565–1576.
- Hawkins, H. F., and D. T. Rubsam, 1968: Hurricane Hilda, 1964. II. Structure and budgets of the hurricane on October 1, 1964. *Mon. Wea. Rev.*, **96**, 617–636.
- , and S. M. Imbembo, 1976: The structure of a small, intense hurricane—Inez, 1966. *Mon. Wea. Rev.*, **104**, 418–442.
- Igau, R. C., M. A. LeMone, and D. Wei, 1999: Updraft and downdraft cores in TOGA COARE: Why so many buoyant downdraft cores? *J. Atmos. Sci.*, **56**, 2232–2245.
- Jordan, C. L., 1961: Marked changes in characteristics of the eye of intense typhoons between the deepening and filling stages. *J. Meteor.*, **18**, 779–789.
- Jorgensen, D. P., 1984a: Mesoscale and convective-scale characteristics of mature hurricanes. Part I: General observations by aircraft. *J. Atmos. Sci.*, **41**, 1268–1285.
- , 1984b: Mesoscale and convective-scale characteristics of mature hurricanes. Part II: Inner core structure of Hurricane Allen (1980). *J. Atmos. Sci.*, **41**, 1287–1311.
- , and M. A. LeMone, 1989: Vertical velocity characteristics of oceanic convection. *J. Atmos. Sci.*, **46**, 621–640.
- , E. J. Zipser, and M. A. LeMone, 1985: Vertical motions in intense hurricanes. *J. Atmos. Sci.*, **42**, 839–856.
- Kossin, J. P., and M. D. Eastin, 2001: Two distinct regimes in the kinematic and thermodynamic structure of the hurricane eye and eyewall. *J. Atmos. Sci.*, **58**, 1079–1090.
- Kuo, H.-L., 1959: Dynamics of convective vortices and eye formation. *The Atmosphere and Sea in Motion*, B. Bolin, Ed., Rockefeller Institute Press, 413–424.
- Lucas, C., E. J. Zipser, and M. A. LeMone, 1994: Vertical velocity in oceanic convection off tropical Australia. *J. Atmos. Sci.*, **51**, 3183–3193.
- Malkus, J. S., 1958: On the structure and maintenance of the mature hurricane eye. *J. Meteor.*, **15**, 337–349.
- , and H. Riehl, 1960: On the dynamics and energy transformations in steady-state hurricanes. *Tellus*, **12**, 1–20.
- Moss, M. S., 1978: Low-layer features of two limited-area hurricane regimes. NOAA Tech. Rep. ERL NHEML-1, 47 pp.
- Ooyama, K. V., 1982: Conceptual evolution of the theory and modeling of the tropical cyclone. *J. Meteor. Soc. Japan*, **60**, 369–380.
- Powell, M. D., 1990: Boundary layer structure and dynamics in outer hurricane rainbands. Part II: Downdraft modification and mixed layer recovery. *Mon. Wea. Rev.*, **118**, 918–938.
- Riehl, H., 1981: Vertical exchange of momentum and energy in the subcloud layer of Australian Hurricane Kerry (1979). *Tellus*, **33**, 105–108.
- Shea, D. J., and W. M. Gray, 1973: The hurricane's inner core region. I. Symmetric and asymmetric structure. *J. Atmos. Sci.*, **30**, 1544–1564.
- Wei, D., A. M. Blyth, and D. J. Raymond, 1998: Buoyancy of convective clouds in TOGA COARE. *J. Atmos. Sci.*, **55**, 3381–3391.
- Willoughby, H. E., 1998: Tropical cyclone eye thermodynamics. *Mon. Wea. Rev.*, **126**, 3053–3067.
- Zhang, D.-L., Y. Liu, and M. K. Yau, 2000: A multiscale numerical study of Hurricane Andrew (1992). Part III: Dynamically induced vertical motion. *Mon. Wea. Rev.*, **128**, 3772–3788.
- Zipser, E. J., R. J. Meitin, and M. A. LeMone, 1981: Mesoscale motion fields associated with a slowly moving GATE convective band. *J. Atmos. Sci.*, **38**, 1725–1750.